**Table IV.** Major Positive Ion Mass Spectral Fragments for $M(Et_2dtc)_3$ Complexes[a]

| probable ion[b] | Co | | Rh | | Ir | |
|---|---|---|---|---|---|---|
| | *m/e* | % *I* | *m/e* | % *I* | *m/e* | % *I* |
| $[ML_3]^+$ | 503 | 7 | 547 | 42 | 637 | 80 |
| $[ML_3 - S_2R]^+$ | 410 | | 454 | | 544 | 10 |
| $[ML_2CS]^+$ | 399 | | 443 | | 533 | 7 |
| $[ML_2S]^+$ | 387 | 10 | 431 | | 521 | 1 |
| $[ML_2]^+$ | 355 | 100 | 399 | 100 | 489 | 31 |
| $[ML_2 - S]^+$ | 323 | 5 | 367 | 34 | 457 | 29 |
| $[ML_2 - S_2]^+$ | 291 | 17 | 335 | 86 | 425 | 52 |
| $[MLS_2]^+$ | 271 | | 315 | 2 | 405 | 13 |
| $[ML_2 - S_2R]^+$ | 262 | 3 | 306 | 1 | 396 | 1 |
| $[MLS]^+$ | 239 | 3 | 283 | 6 | 373 | 8 |
| $[ML]^+$ | 207 | 20 | 251 | 11 | 341 | 2 |
| $[ML - S(\pm H)]^+$ | 175 | 12 | 219 | 30 | 309 | 1 |
| $[MRNCS]^+$ | 146 | 11 | 190 | 4 | 280 | |
| $[ML - CS_2(\pm H)]^+$ | 131 | 1 | 175 | 3 | 265 | |
| $[L(\pm H)]^+$ | 148 | 10 | 148 | 16 | 148 | 5 |
| $[MS_2]^+$ | 123 | 4 | 167 | 14 | 257 | |
| $[L - S]^+$ | 116 | 39 | 116 | 41 | 116 | 69 |
| $[L - SR(\pm H)]^+$ | 87 | 36 | 87 | 66 | 87 | 100 |
| $[L - S_2]^+$ | 84 | | 84 | 4 | 84 | 8 |
| $[L - CS_2]^+$ | 72 | 6 | 72 | 12 | 72 | 14 |
| $[H_2NCS]^+$ | 60 | 14 | 60 | 26 | 60 | 67 |

[a] All spectra recorded under identical instrumental conditions. [b] L = $Et_2NCS_2$, R = Et; Other symbols are defined in Table III.

with both expectation and the electrochemical redox data.

In contrast, the mass spectrometric studies do show the expected trend for the reactivity of the M(IV) state of Co(IV) > Rh(IV) > Ir(IV) (based on the relative abundances of $[M(RR'dtc)_3]^+$) and the inverse order for the reactivities of the lower oxidation states (based on the relative abundances of $[M(RR'dtc)_2]^+$ and $[M(RR'dtc)]^+$). It is believed that the major reason for the differences in the reactivity trends between the electrochemical studies in the solution phase and mass spectrometric studies in the gas phase is that second-order gas-phase dimerization reactions are unfavorable under the conditions of mass spectrometry. Without this pathway, the rhodium(IV) dithiocarbamate complexes have their expected relative reactivities with respect to those of their Co(IV) and Ir(IV) counterparts.

**Table V.** Reversible Half-Wave Potentials ($\approx E^\circ$ values) Calculated from Cyclic Voltammetric Data Obtained at Platinum Electrodes at 20 °C for the Oxidation of $1.0 \times 10^{-3}$ M $M(RR'dtc)_3$ and $M(Et_2dsc)_3$ in Dichloromethane (0.1 M $Bu_4NClO_4$)

| ligand | $E^r_{1/2}$, V[b] | | |
|---|---|---|---|
| | Co | Rh[a] | Ir |
| $Et_2dtc$ | 0.86 | 1.12 | 0.79 |
| *i*-$Pr_2dtc$ | 0.74 | 1.02 | 0.68 |
| Morphdtc | 1.01 | 1.22 | 0.92 |
| Pyrrdtc | 0.90 | 1.11 | 0.81 |
| $Et_2dsc$ | 0.54 | 0.78 | 0.56 |

[a] Data obtained at very fast scan rate.[21] [b] Potential vs Ag/AgCl.

The gas-phase mass spectrometric data as obtained in this work do not provide thermodynamic information that can be correlated with the solution $E^\circ$ data obtained from electrochemical measurements. That is, all the above discussion concerning the comparison between gas and solution results refers to the kinetic reactivity of the $[M(RR'dtc)_3]^+$ and $[M(RR'dsc)_3]^+$ species. In other studies,[34] it has been demonstrated by photoelectron spectroscopy that gas-phase ionization energies of ferrocene derivatives may be correlated with the voltammetric data obtained in the range of solvents. Unfortunately, no ionization potential data are available for the compounds considered in this work, and a thermodynamic correlation cannot be considered.

However, a very recent report[35] has described a correlation between electrochemical oxidation in solution and ionization potential in the gas phase for $(C_5R_5)_2M$ compounds (M = Fe, Ru, Os; R = H, Me). Interestingly, both techniques show the order Fe < Os < Ru for these compounds.

Contribution from the Department of Chemistry, University of British Columbia, Vancouver, BC, Canada V6T 1Y6

# Independence of the Ethylene Ligands in Bis($\eta^2$-ethene)rhodium(I) Complexes

Eugene B. Wickenheiser and William R. Cullen*

*Received December 11, 1989*

A $^1H$ NMR study of bis($\eta^2$-ethene)(2′-acetylphenoxy-*O*,*O*′)rhodium(I) reveals two separate types of exchange processes, namely, ethylene rotation and ethylene dissociation. The exchange processes are studied by using a variety of NMR techniques that allow the calculation of the activation parameters: the ethylene ligands behave independently with respect to both types of exchange.

## Introduction

The study of fluxionality in organometallic molecules provides useful information about the strength and type of interaction between ligand and metal, steric interactions between ligands, and preferred geometries and can lead to predictions of reactivity. NMR studies have revealed a variety of fluxional processes and techniques are available to correlate exchanging nuclei and, more importantly, determine rates of exchange.[1-7] Determination of the exchange rates at a range of temperatures allows the calculation of the activation parameters for the fluxional processes.

Data for the simplest calculation of $\Delta G^\ddagger$ can be acquired from the NMR spectrum at the temperature at which the resonances due to the exchanging nuclei coalesce.[4] More sophisticated methods determine the rate constant $k$ for the fluxional process; the activation parameters can then be calculated by using the Eyring equation. A useful, and more accurate, technique for determining $\Delta G^\ddagger$, first described by Forsen and Hoffman,[8] is spin saturation transfer. In their method a resonance absorption due to one set of the exchanging nuclei is saturated and the decrease in intensity of the resonances due to the nuclei with which it is exchanging is monitored. A disadvantage of this spin saturation

(1) Cramer, R. *J. Am. Chem. Soc.* **1964**, *86*, 217.
(2) Vrieze, K.; Van Leeuwen, P. W. N. M. *Prog. Inorg. Chem.* **1974**, *14*, 1.
(3) Noggle, J. H.; Shirmer, R. E. *The Nuclear Overhauser Effect, Chemical Applications*; Academic: New York, 1971.
(4) Sandstrom, J. *Dynamic NMR Spectroscopy*; Academic Press: New York, 1982.
(5) Martin, M. L.; Martin, G. J.; Delpuech, J. *Practical NMR Spectroscopy*; Heyden and Son: London, 1980.
(6) Jolly, P. W.; Mynott, R. *Adv. Organomet. Chem.* **1981**, *19*, 257.
(7) Stengle, T. R.; Langford, C. H. *Coord. Chem. Rev.* **1967**, *2*, 349.
(8) Forsen, S.; Hoffman, R. A. *J. Chem. Phys.* **1966**, *45*, 2059.

0020-1669/90/1329-4671$02.50/0 © 1990 American Chemical Society

transfer technique is that it is complicated when the exchanging nuclei are coupled because of the presence of the nuclear Overhauser effect (NOE). In systems in which NOE enhancement is expected, it is necessary either to know the exact value of the enhancement factor or to turn to another method such as computer fitting.

The use of dynamic NMR fitting programs gives reasonably accurate values of $k$, which can then be used to calculate the activation parameters. An advantage of the NMR fitting technique is the ability to determine exchange rates that are much higher than those that are accessible by the use of spin saturation transfer; the fitting techniques are capable of determining exchange rates as long as line broadening (due to the exchange) is present. One of the disadvantages of the dynamic NMR fitting programs is that the exchanging system must be well understood. The technique in itself affords little information regarding the exchange process, and it is possible to generate a spectrum resembling the observed spectrum by using improper assumptions regarding the exchange.

Alternative approaches to Forsen and Hoffmann's method for the calculation of $k$ are described by Noggle and Shirmer.[3] These methods offer a means of measuring spin saturation transfer before NOE has made an effect on the magnetization or relaxation of the spin system. The rate constant for the exchange is calculated by two experiments: the first (experiment 1) yields the value of the total direct relaxation rate $R$ and the second (experiment 2) yields a value that is the difference between $R$ and the rate for the exchange.

The present paper is concerned with the application of this approach to study the rotation and ethylene exchange in the molecule bis($\eta^2$-ethene)(2'-acetylphenoxy-$O,O'$)rhodium(I) (**1**).

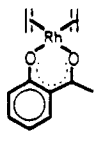

1

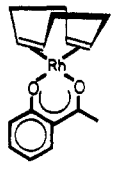

2

## Experimental Section

**Materials.** Rhodium complexes **1** and **2** were synthesized by previously reported methods.[9] The NMR samples employed in this study were prepared by using toluene-$d^8$ as solvent. The toluene was vacuum-transferred to 5-mm NMR tubes containing the sample and was degassed by using several freeze–pump–thaw cycles prior to sealing the tube.

**NMR Measurements.** $^1$H NMR spectra were measured on a Varian XL300 spectrometer (300 MHz) fitted with a variable-temperature apparatus. The error in temperature measurement is $\sim\pm0.1$ °C. The experimental procedures were essentially those described by Noggle and Shirmer.[3] Delay times between scans were set at $5T_1$ values for the observed protons, and evolution periods ($D2$) were varied from zero to a value at which the system had achieved a steady state, by successive trials.

**NMR Simulations.** NMR simulations were carried out by using the dynamic NMR spectra fitting program DNMR3. Coupling constants employed for the ethylene protons were as follows: cis, 8.8 Hz; trans, 13.6 Hz; geminal, −0.060 Hz. The $T_2$ value for the ethylene protons in compound **1** was computed from line widths and was found to be 48 ms. The low exchange limit, or point at which lowering the temperature further will no longer affect the shape of the peaks, was assigned as having an exchange rate equal to 0. The value of the transverse relaxation time was adjusted so that the computer-generated spectra at $k = 0$ would match the low exchange limit spectra. The rest of the computer-generated fits were then made by varying $k$ and correcting for the temperature dependence of the chemical shift.

## Results and Discussion

Complex **1** is suitable for a detailed NMR study because at low temperature the ethylene ligands give rise to well-separated resonances in the $^1$H NMR spectrum. Cramer[1] noted that at low

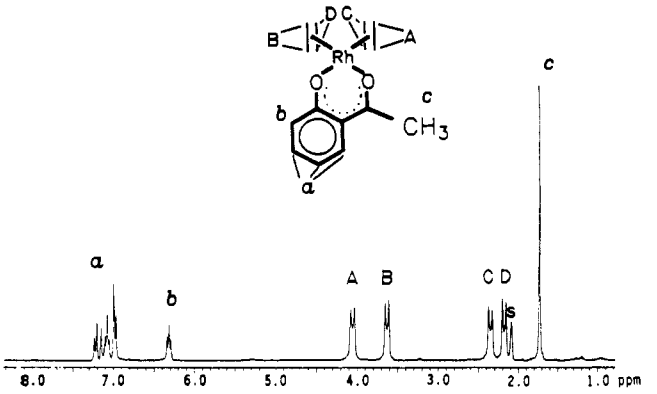


**Figure 1.** $^1$H NMR spectrum of **1** at −56.5 °C. Assignments are as indicated; s = solvent.

temperature the $^1$H NMR spectrum of the symmetrical complex **3** gives rise to two separate resonances associated with the ethylene

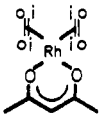


3

ligands. The high-field resonance was assigned to the "inner" ethylene protons (i) and the low-field resonance was assigned to the "outer" ethylene protons (O) as indicated.

The $^1$H NMR spectrum of **1** at −40 °C (Figure 1) reveals two sets of inner and outer protons, one set per ethylene, because of the asymmetric nature of the 2'-hydroxyacetophenone ligand. The ethylene nearest to the deshielding ketone functionality is expected to be shifted further downfield. Another possible rationale for the assignment is the observation that the more strongly bound an ethylene ligand is to the metal center, the higher the resonance will be shifted upfield.[11] In complex **1** it is expected that the ketone oxygen would exert a lower trans effect than the phenoxide oxygen.[12,13] Thus, the ethylene trans to the ketone would be more strongly bound and would appear further upfield in the NMR spectrum. Both of these rationales suggest that the ethylene cis to the ketone (ethylene I) would be the downfield ethylene and the ethylene trans to the ketone, the upfield ethylene (ethylene II).

At room temperature all of the ethylene protons give rise to a single broad resonance. The coupling patterns of each ethylene (Figure 1) can be described as AA'XX'. Assignment of the protons to particular ethylene ligands was made on the basis of decoupling experiments as follows: irradiating the A resonance at 4.05 ppm (AA' of ethylene I) decouples the C resonance at 2.35 ppm (XX' of ethylene I); irradiation of the B resonance at 3.63 ppm (AA' of ethylene II) decouples the D resonance at 2.18 ppm (XX' of ethylene II).

Irradiation of one of the resonances, such as A, also causes a decrease in intensity of the resonance due to the protons on the same ethylene, C, aside from the decoupling effect, due to spin saturation transfer. This effect is apparent at temperatures above −60 °C. Irradiation of A or C also causes a decrease in the intensity of B and D, which are associated with the other ethylene (a decrease in A and C is also noted upon the irradiation of B or D). This saturation transfer effect is less pronounced than that caused by exchange between protons of the same ethylene and is only apparent at temperatures above −45 °C. Two mechanisms

(9) Cullen, W. R.; Wickenheiser, E. B. *J. Organomet. Chem.* **1989**, *370*, 141.
(10) Determined by the inversion-recovery method.
(11) Cramer, R.; Kline, J. B.; Roberts, J. D. *J. Am. Chem. Soc.* **1969**, *91*, 2519.
(12) Tobe, M. L. In *Comprehensive Coordination Chemistry*; Wilkinson, G., Gillard, R. D., McCleverty, J. A., Eds.; Pergamon: New York, 1987; Vol. 1, Chapter 7, p 315.
(13) Bailar, J. C., Jr. In *Comprehensive Coordination Chemistry*; Wilkinson, G., Gillard, R. D., McCleverty, J. A., Eds.; Pergamon: New York, 1987; Vol. 1, Chapter 1, p 21.

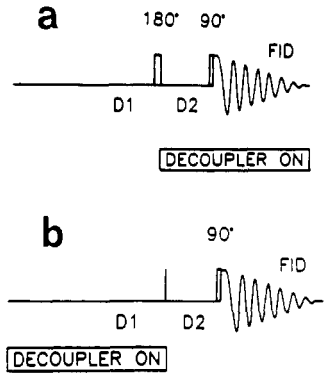


**Figure 2.** (a) Pulse sequence employed for the determination of $R$ and (b) pulse sequence employed for the determination of $\sigma$.

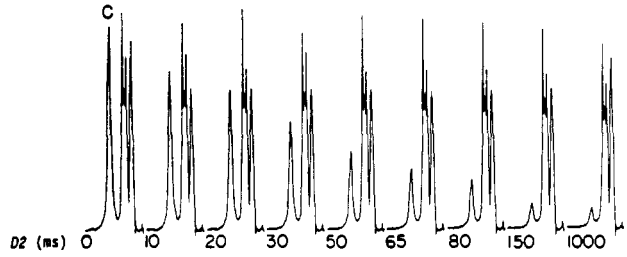


**Figure 3.** Experiment 1, showing the effect of the irradiation of the A protons on the protons (C{A}) at increasing values of $D2$ (ms).

are necessary to account for these observations. Rotation of the ethylene ligands about the rhodium–ethylene bonds exchanges nuclei sets A and C and B and D, accounting for the first type of saturation transfer. Dissociation of ethylene seems to be necessary to account for the second mode of exchange.

**Ethylene Rotation.** As mentioned above, the spin saturation transfer method first described by Forsen and Hoffman[8] is often used for studying the exchange in fluxional molecules. In the absence of NOE effects, this experiment can be applied for the measurement and calculation of the exchange rate $k$ for olefin rotational processes. However, in the case of **1** the coupling interaction in the ethylene ligands implies that NOE will be present during the decoupling of one of the sets of resonances. If NOE is present, the observed resonance will have a higher intensity than expected for a given exchange rate during spin saturation transfer. The presence of NOE will then cause calculated $k$ values to be artificially low. The amount of NOE enhancement present is difficult to quantify, as the longitudinal relaxation rates of the ethylene protons are temperature dependent.[5] The modification described in the Introduction circumvents this problem as follows.

In experiment 1 the total direct relaxation parameter $R$ is measured by the rate of decrease in magnetization of a resonance after instantaneous saturation of the resonance with which it is exchanging. This is achieved experimentally by using the pulse sequence shown in Figure 2a. An example of experiment 1 is shown in Figure 3, where the resonance of **1** at 4.1 ppm has been saturated and the spectrum collected after set time intervals after saturation. The system is described by eq 1, where $\langle I_A \rangle$ = the

$$\langle I_A \rangle = I_{OA} + \left(\frac{\sigma_A}{R_A}\right) I_{OB}(1 - e^{-R_A}) \qquad (1)$$

magnetization of nuclei A, as measured in the $z$ direction, at time $t$, $I_{OA}$ = the equilibrium magnetization of nuclei A, $I_{OB}$ = the equilibrium magnetization of nuclei B, $\sigma_A$ = the cross-relaxational parameter measured from nuclei A during the irradiation of nuclei B, $R_A$ = the total relaxation parameter of nuclei A, and $t$ = time (seconds). The value of $R$ is calculated from the slope of the plot of ln $(I - I_\infty)$ versus time ($R$ = −slope). The time allowed before data collection ($D2$) varies from 0 to a value that is less than the time required for NOE to build up; this period is illustrated in the plot of ln $(I - I_\infty)$ versus time (Figure 4). This plot represents the effect of the instantaneous saturation on the set of nuclei with

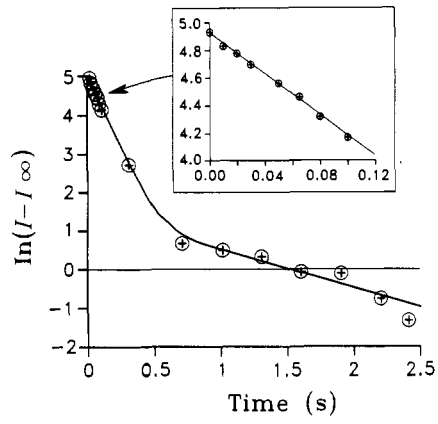


**Figure 4.** Plots of ln $(I - I_\infty)$ versus $D2$ (s) for C{A} at −38.5 °C. The upper plot is an expansion of the left side of the bottom plot.

**Table I.** Activation Parameters Calculated for Ethylene Rotation[a]

| | $\Delta H^\ddagger$, cal/mol | $\Delta S^\ddagger$, cal/(mol K) | $\Delta G^\ddagger$, kcal/mol |
|---|---|---|---|
| | Saturation Transfer | | |
| ethylene I | 14.7 (0.2) | 10.8 (0.8) | 11.8 (0.03) |
| ethylene II | 14.7 (0.7) | 7.91 (3.04) | 12.5 (0.1) |
| | DNMR3 | | |
| ethylene I | 13.5 (0.3) | 5.50 (1.19) | 12.0 (0.04) |
| ethylene II | 13.4 (0.6) | 2.42 (2.66) | 12.7 (0.08) |

[a] Standard deviations in parentheses.

which the irradiated nuclei are exchanging at specific time intervals after initial saturation. The experiment was performed at −38.5 °C. The initial slope, upper plot, is equal to $-R$ and the lower curve shows the effect of $R$, initially, and $R$ and NOE, later.

Values of the cross-relaxation time $\sigma_{AB}$ ($\sigma_{AB} = -k_{exchange}$) in the absence of NOE are obtained from the equilibrium magnetization of the observed spin, which equals $I_{OA} + I_{OB}(\sigma_{AB}/R_A)$. However, in **1** the equilibrium magnetization reflects both $\sigma_{AB}/R_A$ and NOE so that $k$ cannot be acquired from this experiment alone.

With the values of $R$ having been determined from experiment 1, the exchange rates are then obtained by performing experiment 2. This experiment affords values for the sum of $R + \sigma$ for the ethylene protons. Here one of the resonances is irradiated until the steady state is reached. The decoupler is then turned off, and the resonances are monitored as they approach their equilibrium magnetizations. This is achieved experimentally by using the pulse sequence shown in Figure 2b; the system is now described by eq 2.

$$\langle I_A \rangle = I_{OA} + C_1 e^{-\lambda_1 t} + C_2 e^{-\lambda_2 t} \qquad (2)$$

$$C_1 = I_{OA}\left(\frac{\sigma_{AB} - \sigma_{BA}}{\lambda_2 - \lambda_1}\right) + I_{OA}\frac{\sigma_{BA}}{R_B}\left(\frac{\lambda_2}{\lambda_2 - \lambda_1}\right)$$

$$C_2 = -I_{OA}\left(\frac{\sigma_{AB} - \sigma_{BA}}{\lambda_2 - \lambda_1}\right) - I_{OA}\frac{\sigma_{BA}}{R_B}\left(\frac{\lambda_1}{\lambda_2 - \lambda_1}\right)$$

$$\lambda_1 = \tfrac{1}{2}\{(R_A - R_B) + [(R_A - R_B)^2 + 4\sigma_{AB}\sigma_{BA}]^{1/2}\}$$

$$\lambda_2 = \tfrac{1}{2}\{(R_A - R_B) - [(R_A - R_B)^2 + 4\sigma_{AB}\sigma_{BA}]^{1/2}\}$$

$$R_A \approx R_B \qquad \sigma_{AB} = \sigma_{BA} \qquad \lambda_1 = R + \sigma \qquad \lambda_2 = R - \sigma$$

At higher exchange rates the slope of ln $(I_A - I_{OA})$ versus time equals $R_A + \sigma_{AB}$ (from eq 2), as $R_A - \sigma_{AB}$ is very small compared to $R_A + \sigma_{AB}$.

The cross-relaxational constant $(-k)$ is obtained by the difference between the slopes of the plots in experiment 1 and experiment 2 ($\sigma_{AB}$ = ($R_A + \sigma_{AB}$(experiment 2)) − $R$(experiment 1) = $-k$). The activation parameters $\Delta H^\ddagger$, $\Delta S^\ddagger$, and $\Delta G^\ddagger$ values are then calculated from the plot of ln $(k/T)$ versus $1/T$.

Plots of ln $(k/T)$ versus $1/T$ for the exchange of protons A and C (ethylene I rotation) and protons B and D (ethylene II rotation)

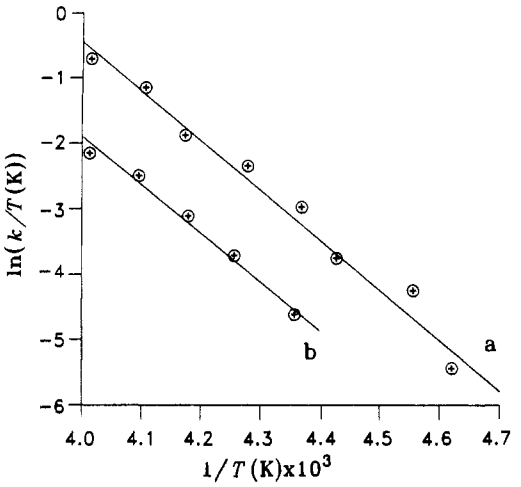


**Figure 5.** (a) ln $(k_{AC}/T)$ versus $1/T$ and (b) ln $(k_{BD}/T)$ versus $1/T$. Data are from spin saturation transfer experiments.

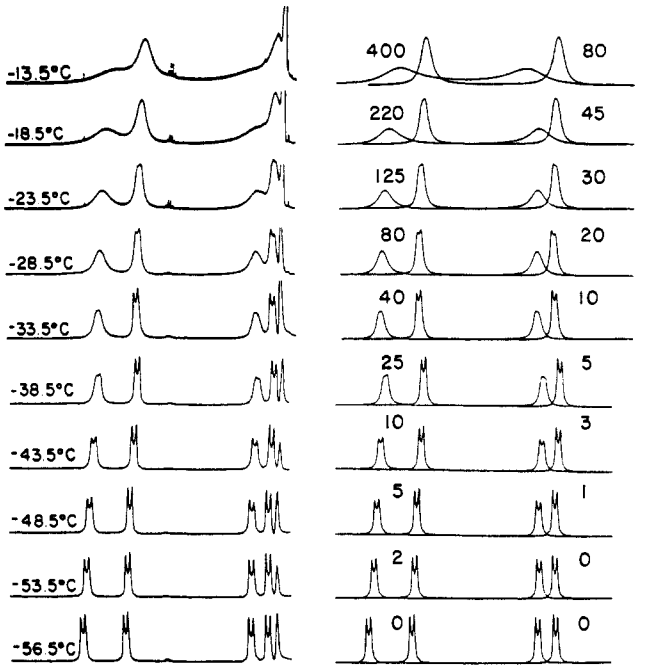


**Figure 6.** Observed variable-temperature $^1$H NMR spectrum of the ethylene resonances in **1** (left) and DNMR3-generated spectrum (right). $k$ values ($s^{-1}$) for rotation of the two ligands are shown.

are shown in Figure 5. The corresponding activation parameters for the processes, calculated from the plots, are displayed in Table I.

**Dynamic NMR Computer Fitting.** Values for the exchange constant were obtained by generating spectra to fit the variable spectra by use of the computer program DNMR3.[4,14-16] If the ethylene ligands are modeled separately, a very satisfactory agreement can be obtained by superimposing the two calculated spectra. A comparison between the experimentally obtained spectra and the computer-generated fits is shown in Figure 6. The trans coupling constants were measured from spectra acquired at the low exchange limit. Values for cis and geminal coupling constants were used as determined by Cramer[11] for the bis($\eta^2$-ethene)($\eta^5$-cyclopentadiene)rhodium(I) complex because the values were not measurable from the obtained spectra of **1** but undoubtedly contributed to line broadening. The values of $k$ used in the calculation of the activation parameters were chosen from

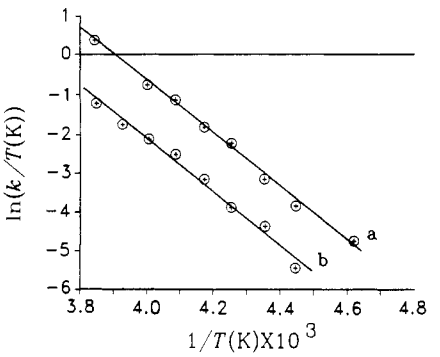


**Figure 7.** (a) ln $(k_{AC}/T)$ versus $1/T$ and (b) ln $(k_{BD}/T)$ versus $1/T$. Data are from dynamic simulation (DNMR3) experiments.

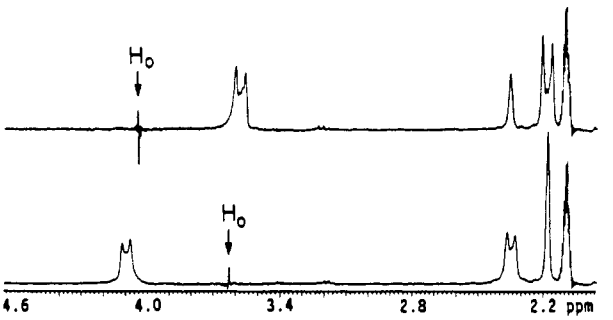


**Figure 8.** Effects of irradiation of A on resonances B and D (top) and effects of irradiation of B on resonances A and C (bottom) at −48.5 °C.

computer-generated spectra showing the best agreement with the experimentally observed spectra. Appropriate plots of ln $(k/T)$ versus $1/T$ are shown in Figure 7. The corresponding activation parameters are listed in Table I.

The activation parameters in Table I do not show a significant difference between $\Delta H^\ddagger$ and $\Delta S^\ddagger$ for rotation of the two ethylenes in data obtained by using the saturation transfer experiments and computer fitting; $\Delta G^\ddagger$ does show a significant difference. The calculated $\Delta G^\ddagger$ is inherently more accurate by virtue of the covariance of $\Delta H^\ddagger$ and $\Delta S^\ddagger$.[17]

Calculated $\Delta G^\ddagger$ values for the separate ethylene ligand rotations for the system at 0 °C[18] show agreement between the DNMR3 results and those obtained from spin saturation transfer experiments. The $\Delta G^\ddagger$ values also distinguish between ethylenes; ligand I (containing resonance groups A and C) has a lower energy barrier for rotation than ligand II (containing resonance groups B and D). These values are in agreement with the observation that the resonances due to ethylene II are resolved at higher temperatures than the ethylene I resonances, and are consistent with the assignment of ligand I to the site trans to the phenoxide oxygen (of higher trans influence) and cis to the ketone donor (of lower trans influence).[12,13]

The activation parameters determined here are in line with others found in related systems. For example, a variety of bis($\eta^2$-olefin)(2,4-pentanedionato-*O*,*O*')rhodium(I) complexes were prepared and their fluxionality studied by Herberhold et al.[19] The calculated $\Delta G^\ddagger$ values for olefin rotations vary from 11.7 kcal/mol for the ethylene ligands in ($\eta^2$-*cis*-dimethoxyethene)($\eta^2$-

(14) Eaton, S. S.; Hutchinson, J. R.; Holm, R. H.; Muetterties, E. L. *J. Am. Chem. Soc.* **1972**, *94*, 6411.
(15) Gordon, J. G.; Holm, R. A. *J. Am. Chem. Soc.* **1970**, *92*, 5319.
(16) Allerhand, A.; Gutowsky, H. S.; Jonas, J.; Meinzer, R. A. *J. Am. Chem. Soc.* **1966**, *88*, 3185.

(17) The errors in $H$ and $S$ are estimated by the calculation of the standard deviations ($\sigma$) in the slope and $y$ intercept in the plot of ln $(k/T)$ versus $1/T$, from which the activation parameters were derived. The standard deviation in $\Delta G^\ddagger$ is relatively lower than that of its constituent $\Delta H^\ddagger$ and $\Delta S^\ddagger$ values due to the covariance between these components. The standard deviation for $\Delta G_T^\ddagger$ is calculated by the following relation, where the error lost in $\Delta G_T^\ddagger$ due to the covariance of $\Delta G^\ddagger$ and $\Delta S^\ddagger$ is reflected in the negative term:

$$(\sigma_{\Delta G_T^\ddagger})^2 = (\sigma_{\Delta H^\ddagger})^2 + (T\sigma_{\Delta S^\ddagger})^2 - 2T\sigma_{\Delta H^\ddagger}\sigma_{\Delta S^\ddagger}$$

(18) The coalescence point is estimated to occur at 0 °C.
(19) Herberhold, M.; Kreiter, C. G.; Wiedersatz, G. O. *J. Organomet. Chem.* **1976**, *120*, 103.

ethene)(acetylacetonato)rhodium(I) to 18.5 kcal/mol for the ligands in ($\eta^2$-2,4-dimethoxy-2-butene)($\eta^2$-ethene)(acetylacetonato)rhodium(I) (**4**). The authors also invoked a "Berry pseudorotation" to account for the coalescence of the resonances of the pentanedione methyl groups at higher temperatures in **4** and bis($\eta^2$-*cis*-methoxyethene)(acetylacetonato)rhodium(I) (**5**).[20] Values of $\Delta G^*$ for the motion were calculated to be 13.9 (**4**) and 15.2 kcal/mol (**5**).[19] Others have invoked pseudorotation to account for the spectra of related four-coordinate rhodium complexes;[21-23] this is discussed further below.

Five-coordinate complexes of $d^8$ metals can undergo concerted ligand rotation and Berry pseudorotation,[24,25] and one study[26] on rhodium(I) complexes lists $\Delta G^*$ values for the coupled process in the range 10.9–18.4 kcal/mol. The activation energy estimated for ethylene rotation in these complexes is 32 kcal/mol; when the concerted pseudorotation is added, the estimated activation energy for the entire process drops to 10 kcal/mol,[27] a value that is in agreement with the experimental results.

**Ethylene Exchange.** Irradiation of one of the proton resonances of one of the ethylene ligands of **1** causes the resonances of the other ligand to decrease in intensity. This effect is displayed in Figure 8, where irradiation of the resonance A at 4.1 ppm, due to the outer protons on ligand I, causes a decrease in the C (3.7 ppm) resonance (due to the ethylene rotation) but also causes a decrease in resonances B (2.4 ppm) and D (2.2 ppm). The decrease in B and D upon the irradiation of A is indicative of exchange between ethylene ligands. The amount of this decrease can be used to calculate the exchange rate. The necessary data can be obtained from experiment I, which was used for the determination of $R$ for ethylene rotation. Here NOE is no longer a factor as the protons on separate ethylene ligands are not coupled to each other. Again $R$ is calculated from the slope of the ln ($I_t - I_\infty$) versus time plot. In this experiment the protons in an ethylene ligand are observed at various times after a set of protons on the other ethylene ligand is saturated. In the absence of NOE it is possible to obtain the ratio $\sigma/R$ from the steady-state magnetization ($I_{OA} + I_{OB}(\sigma_{AB}/R_A)$; $I_{OA} = I_{OB}$). The rate of exchange of the two ligands is not the same; irradiation of a set of protons on ethylene II causes a greater decrease in the intensity of the ethylene I resonances than vice versa; this effect is evident in the variable-temperature decoupled spectra, in Figure 8. Saturating the B resonance has a much greater effect on resonances A and C than the effect of saturating the A resonance has on B and D. Saturation of the B resonance effects the complete saturation of A and C resonances at a temperature of −28.5 °C. A temperature of higher than −23.5 °C is required for the irradiation of A to completely saturate B and D.

Intramolecular exchange by Berry pseudorotation, described above, does not seem to be occurring here. The difference in the values of $k_{B|A|}$ (rate of exchange calculated for B during the irradiation of A) and $k_{A|B|}$ (obtained during irradiation of B) indicates that the exchange between ethylenes is not intramolecular; otherwise the observed rates would be equal. An intermolecular process involving the collision of two molecules of complex and exchange of ethylene also does not account for the disparity in the observed exchange rates as, again, they are expected to be equal. Further evidence negating this type of exchange is garnered from the study of the COD analogue of **1**, complex **2**, described next.

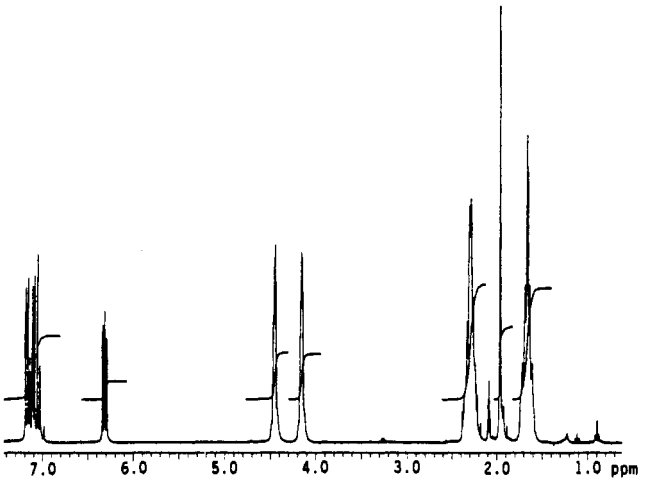


**Figure 9.** $^1$H NMR spectrum of **2** at room temperature.

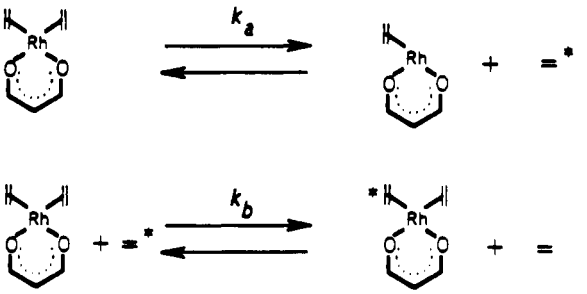


**Figure 10.** Mechanism of intermolecular ethylene exchange.

The COD analogue of **1** is an ideal model for the study of the possibility of intramolecular exchange in complexes of this type. It is expected that if a Berry pseudorotation process is occurring in **1**, it should also occur in **2**. The $^1$H NMR spectrum of **2** at room temperature is shown in Figure 9. One of the advantages of using complex **2** is that it has only two, well-separated, resonances for the olefinic protons in the $^1$H NMR spectrum. Another feature of this system is that the olefinic protons are not coupled to each other. This feature should allow easy study of exchange by using the spin saturation transfer method, since NOE should not be a problem. Variable-temperature $^1$NMR spectra of **2** run at temperatures ranging from +30 to −30 °C show no changes associated with an exchanging system; this implies the absence of exchange between the olefinic protons. Similarly, no intramolecular exchange should occur between the ethylene ligands of **1**. The ethylene exchange can then be addressed as an intermolecular process.

The position of the olefinic proton resonances in the spectrum of **2** (4.13, 4.43 ppm) support the assignment of the ethylene resonances in the low-temperature $^1$H NMR spectrum of **1**. The olefinic protons in **2** are structurally analogous to the "outer" protons in **1**, as COD has no "inner" protons, and lie in the same region in the NMR spectrum (the outer ethylene protons appear at 3.5 and 4.2 ppm in **1**). The shielding effect of the COD backbone upon the olefinic protons in **2** is expected to be negligible.

The mechanism of the ethylene exchange in **1** appears to involve free ethylene and the 16-electron bis(ethene)rhodium(I) complex. A schematic representation of the proposed reaction mechanism is shown in Figure 10. The first step in the reaction is the dissociation of ethylene; this process must be reversible, because no decomposition or change in the $^1$H NMR spectrum is observed over long periods. The presence of any significant amount of ethylene in solution would give rise to a peak in the NMR spectrum unless if it were undergoing rapid exchange. If free ethylene were present and rapid exchange were occurring, the

(20) Maisonant, A.; Poilblanc, R. *Inorg. Chim. Acta* **1978**, *29*, 203. Bis($\eta^2$-ethene)(2,6-lutidine-*N*)rhodium(I) chloride exhibits a $^1$H NMR spectrum indicative of two chemically and magnetically inequivalent ethylene ligands. The study of this and other complexes lead the authors to suggest the possibility of a "gear mechanism" that couples the motion of the ethylene ligands, allowing them to rotate only at similar rates; the present results seem to negate this postulate.
(21) Chen, M. J.; Feder, H. M. *Inorg. Chem.* **1979**, *18*, 1864.
(22) Reis, A. H.; Willi, C.; Siegel, S.; Tani, B. *Inorg. Chem.* **1979**, *18*, 1859.
(23) Cocivera, M.; Ferguson, G.; Lalor, F. J.; Szczecinski, P. *Organometallics* **1982**, *1*, 1139.
(24) Kaneshima, T.; Kawakami, K.; Tanaka, T. *Inorg. Chim. Acta* **1975**, *15*, 161.
(25) Hogeveen, H.; Nusse, B. J. *J. Organomet. Chem.* **1979**, *171*, 237.
(26) Kaneshima, T.; Yumoto, Y.; Kawakami, K.; Tanaka, T. *Inorg. Chim. Acta* **1976**, *18*, 29.
(27) Albright, T. A.; Hoffmann, R.; Thibeault, J. C.; Thorn, D. L. *J. Am. Chem. Soc.* **1979**, *101*, 3801.

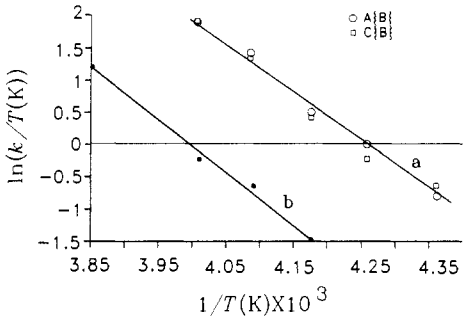


**Figure 11.** (a) Plot of ln $(k/T)$ versus $1/T$ for exchange of ethylene I and (b) plot of ln $(k/T)$ versus $1/T$ for exchange of ethylene II.

resonances due to the protons with which it was exchanging (i.e. the ethylene ligand protons) would be shifted downfield toward the position of free ethylene; also, the chemical shift for the ethylene ligand resonances would be temperature dependent. Neither of these effects are observable, indicating that the equilibrium for the dissociative reaction favors the 16-electron complex.[28]

The second step of the overall process involves the reaction between ethylene and either a 16-electron complex or a 14-electron intermediate. If the ethylene associates to a vacant site on a 14-electron intermediate, the association will only be observable if it involves ethylene site exchange (i.e. ethylene going from site I to site II or from site II to site I). This selective measurement results from the experimental method in which spin saturation transfer can only be attributed to exchange with the second type of ethylene ligand (the one being saturated). The favored reaction, between ethylene and the 16-electron complex, appears to proceed via a five-coordinated intermediate, since the equilibrium lies toward the associated complex. Such an intermediate has been postulated for the exchange reaction between gaseous ethylene and bis($\eta^2$-ethene)(2,4-pentanedionato-*O*,*O*')rhodium(I).[1] The exchange can then be explained by dissociation of one of the ethylene ligands from the five-coordinate complex and migration of the "new" ethylene into the vacant site.

(28) When the spectrum of **1** is measured in the presence of 1 atm of ethylene (60 Torr), no significant differences from the normal spectrum are observed in the bound ethylene region over the temperature range −32.5 to −65 °C.

**Table II.** Calculated Activation Parameters for Dissociation[a]

| | ethylene I | ethylene II |
|---|---|---|
| $\Delta H^{\ddagger}$, kcal/mol | 15.5 (0.7) | 16.1 (0.9) |
| $\Delta S^{\ddagger}$, cal/(mol K) | 18.9 (2.7) | 16.9 (3.8) |
| $\Delta G_{300K}{}^{\ddagger}$, kcal/mol | 9.83 (0.17) | 11.0 (0.2) |

[a] Standard deviations in parentheses.

The magnetization of the ethylene in one of the sites is monitored during saturation of the ethylene in the other site. The concentration of complex with the ligand associated at that site is proportional to the magnetization. A decrease in magnetization at the monitored sites is caused by exchange with a saturated ligand (indicated by an asterisk) or by dissociation (Figure 10). The rate of decrease in the concentration of associated ligand in one site is given by eq 3; because [ethylene] ≪ [complex], the second term can be ignored and the rate law becomes eq 4.

$$-\frac{\mathrm{d(observed\ species)}}{\mathrm{d}t} = k_a[\mathrm{complex}] + k_b[\mathrm{ethylene}][\mathrm{complex}] \quad (3)$$

$$-\frac{\mathrm{d(observed\ species)}}{\mathrm{d}t} = k_a[\mathrm{complex}] \quad (4)$$

The rate constant for the exchange ($k_a$) is equal to $k/[\mathrm{complex}]$ ([complex] = 0.016 M). It was not possible to acquire data by observation of the D protons, as too much overlap with the solvent peak occurs at these temperatures. Plots of ln $(k/T)$ are shown in Figure 11. Again the activation parameters were calculated from the slope and $y$ intercept from these plots. Error calculations were also performed as previously described; a single error calculation is performed for observation of A and C exchange, as the intermolecular exchange does not discriminate between ethylene sites on individual ethylene ligands. Activation parameters are shown in Table II.

The results of the study of the intermolecular exchange are consistent with those for ethylene rotation. In both cases ethylene I is undergoing more rapid exchange with lower activation barriers to the motion than ethylene II. The ethylene trans to the $\sigma$-bound oxygen (ethylene I) has the lower activation barrier for the dissociation reaction, which is as expected.

**Acknowledgment.** We thank the Natural Sciences and Engineering Research Council of Canada for financial support.